

A search for ferromagnetism in transition-metal-doped piezoelectric ZnO

Nicola A. Spaldin
Materials Department, University of California,
Santa Barbara, CA 93106-5050

May 26, 2020

Abstract

We present the results of a computational study of ZnO in the presence of Co and Mn substitutional impurities. The goal of our work is to identify potential ferromagnetic ground states within the (Zn,Co)O or (Zn,Mn)O material systems that are also good candidates for piezoelectricity. We find that, in contrast to previous results, robust ferromagnetism is not obtained by substitution of Co or Mn on the Zn site, unless additional carriers (holes) are also incorporated. We propose a practical scheme for achieving such *p*-type doping in ZnO.

1 Introduction

The observation of ferromagnetism in diluted magnetic semiconductors such as (Ga,Mn)As[1] has spawned a great deal of recent research in the field now popularly known as “spintronics” [2]. Indeed a room temperature magnetic semiconductor is likely essential for the development of commercial spintronic devices, such as spin valves and transistors, which exploit the fact that electrons have *spin* as well as charge.

There has been similar recent activity in the field of “multifunctional”, or “smart” materials, which encompasses piezoelectrics, magnetostrictive materials, shape memory alloys, and piezomagnetic materials, to name a few. The progress has been driven in part by their application in micro-electromechanical and nano-electromechanical systems (MEMS and NEMS) which are integrated micro-devices or systems combining electrical and mechanical components as sensors and actuators. Piezoelectric materials are of particular interest, both because of their fascinating fundamental physics and for their utility as transducers between electrical and mechanical energy. Applications are diverse and include medical ultrasound devices, smart structures in automobiles, naval sonar and micromachines.

This paper describes a computational study of one possible avenue for *integration* of the fields of spintronics and smart materials: the design of a piezoelectric semiconductor-based ferromagnet. Many potential device applications can be envisaged for such a material including electric field or stress-controlled ferromagnetic resonance devices, and variable transducers with magnetically modulated piezoelectricity [3]. Also, the ability to couple with *either* the magnetic *or* the electric polarization offers additional flexibility in the design of conventional actuators, transducers and storage devices. However the relationship between ferromagnetism and piezoelectricity has not, to our knowledge, been explored previously.

The material system that we focus on here is transition metal doped ZnO, in which the transition metal is incorporated substitutionally at the Zn site. This has been the subject of a number of recent experimental studies focussed on the magnetic properties, following a prediction using a simple mean field model that *p*-doped samples should have a high ferromagnetic Curie temperature[4]. While the most recent work on well-characterized (Zn,Co)O samples indicated antiferromagnetic coupling between the Co ions[5] there have also been a number of earlier reports of possible ferromagnetism. For example Ueda *et al.* [8] reported that pulsed laser deposition (PLD) grown films of (Zn,Co)O with Co concentrations between 5 and 25 % displayed Curie temperatures between 280 K and 300 K, with a saturation magnetization between 1.8 and 2.0 μ_B per Co. They suggested that in addition to possible “intrinsic” ferromagnetism from (Zn,Co)O, perhaps in the presence of hole carriers, the presence of cobalt oxide grains might also account for the observed behavior. Kim *et al.* [9] also used PLD to grow (Zn,Co)O films and found evidence for ferromagnetism when the films were grown under low O₂ partial pressure. The origin of the ferromagnetism was not “intrinsic” however, but resulted from the formation of cobalt microclusters. Finally, Lim *et*

al. [11] reported ferromagnetism in $\text{Zn}_{1-x}\text{Co}_x\text{O}$ ($0.02 \leq x \leq 0.40$) films grown by magnetron co-sputtering on sapphire. Other evidence for magnetic phenomena include observation of a large magnetic circular dichroism signal at an energy corresponding to the ZnO band edge in thin films of ZnO doped with Mn, Co, Ni and Cu [6, 7]. This indicated significant influence of the transition metal on the ZnO states. Also optical studies on laser ZnO:Co films (with some Al) on sapphire confirmed that Co was divalent, high spin, and substituting for Zn[10].

In addition to the proposed applications exploiting the magnetic semiconducting behavior, a ZnO-based system has a number of other potential applications. First it suggests the possibility of fabricating a *transparent* ferromagnet that will have great impact on industrial applications, for example in magneto-optical devices. Also, since the host ZnO material crystallizes in the wurtzite structure and is piezoelectric, we believe that transition metal doped ZnO is a promising system for designing the first ferromagnetic piezoelectrics. Piezoelectricity in transition metal doped ZnO has not been explored to date.

In this paper we explore computationally the effects of doping a ZnO host with two transition metals (Mn and Co) over a range of concentrations, and containing impurities that are likely to occur in such systems. By calculating the relative stability of the magnetic phases of the candidate materials, we identify those with the strongest ferromagnetic tendencies, and by inspecting the band structures we assess the most promising for piezoelectricity. Previous authors have used density functional calculations to predict magnetic ground states in such systems. Sato and Katayama-Yoshida [12] predicted that, within the Korringa-Kohn-Rostoker and local spin density approximations, a ferromagnetic ground state would be favored at 25%-doping for most $3d$ transition metals. For Mn-substitution they predicted that hole doping would induce ferromagnetism. The same authors have recently extended their study to lower transition metal concentrations using the coherent potential approximation to model the dilute alloy, and reached the same conclusions [13]. The main result of our work, however, is that ferromagnetism is in general *not* strongly favored in ZnO doped with either Co or Mn, unless additional dopants which provide p -type carriers are also present.

The remainder of this paper is organized as follows. In the next Section we describe the technical details for the calculations performed in this work. In Section 3 we describe our results for (Zn,Mn)O and (Zn,Co)O, as well as the intriguing possibility of creating a ferromagnet using only vacancy doping. Finally, in Section 4 we present our conclusions and propose a practical scheme for creating a robust ZnO-based ferromagnet.

2 Computational Details

2.1 SIESTA

In order to simulate realistic dopant concentrations, we need to perform calculations for supercells containing a large number of atoms. Therefore we use a density functional theory (DFT) approach based on pseudopotentials with localized atomic orbital basis sets. This method, implemented in the code SIESTA [14, 15, 16], combines accuracy with small computational cost, particularly compared to other approaches such as plane wave pseudopotential or all-electron methods. For a comprehensive description of the SIESTA program, and its use in understanding the properties of related systems, see in particular Refs. [15] and [17]. Our pseudopotentials are designed using the standard Troullier-Martins formalism [18] with non-linear core corrections [19] and Kleinman-Bylander factorization [20]. We use the Ceperley-Alder local spin density (LSDA) exchange-correlation functional [21], and include scalar relativistic effects for Mn, Co and Zn. For Zn, we include the $(3d)^{10}$ electrons in the valence manifold, and construct the pseudopotential using a Zn^{2+} reference configuration with cut-off radii (r_{cs}) of 2.0, 2.1 and 1.9 a.u. for the $4s$, $4p$ and $3d$ orbitals respectively, and a partial core radius of 0.6 a.u. The eigenvalues and excitation energies of related configurations calculated from this pseudopotential agreed with the all-electron values to within 4 mRy, and the bulk lattice constants, atomic positions and band structures (calculated using maximal basis sets) were in good agreement with all-electron values [22]. We use the Mn pseudopotential of Refs. [24] and [17], which has been extensively tested in calculations for MnAs and (Ga,Mn)As. The reference configuration was $4s^2 4p^0 3d^5$ with cut-off radii for the s , p and d components of 2.00, 2.20 and 1.90 au respectively. The Co pseudopotential, constructed from a $4s^1 3d^8$ reference configuration, r_{cs} of 2.0 a.u. for all valence orbitals and a partial core cut-off of 0.75 a.u., was previously tested for Co metal and shown to give good agreement with all-electron LSDA lattice constants[28, 29]. The oxygen pseudopotential was constructed from a $2s^2 2p^4$ reference configuration, r_{cs} of 1.15 a.u. for each angular momentum channel and no core corrections. Eigenvalues and excitation energies for related atomic states agreed within 1 mRy of the all-electron values. The oxygen pseudopotential has also been tested extensively in calculations for bulk oxides[30].

In localized orbital calculations, care must also be taken in the optimization of the basis set. The procedure to generate the numerical atomic orbital basis is described in Ref. [27]. Several parameters determine the accuracy of the basis, including the number of basis functions, the angular momentum components included and the confinement radii. All these have been optimized here to achieve the required accuracy. The calculated structural and electronic properties of ZnO were largely unchanged on reducing from the maximal basis to two unpolarized basis functions (ζ s) per orbital, therefore we decided to use such a double- ζ basis for each Zn and O orbital. Since we are primarily interested in the magnetic properties of diluted systems which contain a small number of magnetic ions, we followed Ref. [17] in

using a triple- ζ basis for the d orbitals on Co and Mn. Note that we can afford to use triple- ζ for Co and Mn d since there are only a small number of these ions in the unit cell. In contrast the use of larger basis sets for Zn and O yields a more dramatic increase of the size of the computations. For the atomic orbital confinement radii we use the well-tested values from Ref. [17] of 6.0, 6.0 and 5.0 a.u. for the Mn s , p and d orbitals. Use of the Mn values for Zn and Co, combined with 5.5 a.u. for O s and p orbitals, gave energy differences between ferro- and anti-ferromagnetic states that agreed well with those for larger confinement radii, while maintaining a reasonable computation time.

Other computational details include a $4 \times 4 \times 3$ Monkhorst Pack grid for 32 atom total energy calculations, with a $10 \times 10 \times 8$ interpolation for density of states calculations, a real space mesh cut-off of 180 Ry and the neglect of non-overlap interactions.

3 Origin and optimization of ferromagnetism in transition-metal doped ZnO.

We begin by performing DFT calculations for bulk (Zn,Mn)O and (Zn,Co)O to search for the presence of ferromagnetism, and to determine the nature of the interactions driving the magnetic ordering. We choose Co as a prototypical dopant since the only current experimental report of ferromagnetism in a ZnO-based system is in Co-doped ZnO films. Mn is attractive for our theoretical studies, since the half-filled $3d$ band of the Mn^{2+} ion might lead to more straightforward interactions in the (Zn,Mn)O band structure.

3.1 (Zn,Mn)O

First we calculate the electronic properties of a 32 atom wurtzite structure supercell of ZnO containing 1 Mn atom substituted at a Zn site. The supercell is formed by doubling the conventional four atom wurtzite structure along each axis and the experimental lattice constant is adopted, giving lattice vectors

$$\begin{array}{ccc} 0.500 & -0.866 & 0.0000 \\ 0.500 & 0.866 & 0.0000 \\ 0.000 & 0.000 & 1.6024 \end{array}$$

and a lattice constant of 12.28 a.u. Note that we do not perform a structural optimization of the atomic positions, since the forces on the atoms in this ideal structure are not large. Since only 1 Mn atom is included in each supercell the overall magnetic ordering is constrained

to be ferromagnetic, and the concentration of Mn ions is 6.25 %. We obtain a calculated magnetic moment of $4.9 \mu_B$ per unit cell, close to the value of $5.0 \mu_B$ predicted for purely ionic Mn^{2+} with five unpaired $3d$ electrons.

Our calculated total density of states for this system is shown as the thin solid line in Figure 1. The majority (up) spin states are plotted along the positive y direction, and the minority (down) spin along negative y , with the pure ZnO density of states shown as the dotted line in the $+y$ direction for comparison. The dashed line shows the energy of the highest occupied state, which we have set to 0 eV. Note that the density of states of Mn-doped ZnO is largely similar to that of undoped ZnO. The Zn d states are concentrated within a largely unpolarized region centered around -7 eV with a dispersion of about 2 eV, and the oxygen p states are found in the region between -6 eV and -2 eV. This is in good agreement with other LDA calculations[22], but with respect to experimental photoemission spectroscopy[23], the $3d$ bands calculated within LDA are too high in energy and overlap with the sp^3 valence band manifold. This causes an overestimation of the Zn $3d$ - O $2p$ hybridization [25] which also shrinks the energy range of the sp^3 bands. The Mulliken population analyses indicate hybridization between the oxygen $2p$ electrons and the cations which is clearly significant in spite of the overestimation. The Zn up and down spin occupations are each 5.45 per atom (they would be 5.0 for a purely ionic Zn^{2+} ion) while those of O are 3.55 per atom (compared to the ionic value of 4.0), indicating electron transfer out of the O^{2-} ion and onto the Zn ions.

The Mn d states (shaded gray, with a thick solid line) are largely localized within the band gap region. The Mn d manifold is split by an exchange splitting of around 4 eV into distinct groups of up-spin and down-spin states, each of which in turn is split by the smaller crystal field splitting (around 1 eV) into the (lower energy) doublet e and higher energy triplet t states. The up-spin Mn states form an impurity state just at the top of the valence band edge which is completely filled. The down-spin states are slightly broadened by overlap with the Zn s states at the bottom of the conduction band. Both up- and down-spin Mn occupations are increased over their purely ionic values (which would be 5.0 and 0.0 respectively) to 5.30 (due to occupation of the up-spin Mn $4s$ orbitals) and 0.75 (due to occupation of both the down spin $4s$ and $3d$).

Finally note that the LDA fundamental energy gap is underestimated by ~ 40 % compared with experiment. This results in a non-zero density of states at the Fermi energy, with the bottom of the Zn $4s$ conduction band overlapping slightly with the top of the up-spin Mn $3d$ states. Although this is likely an artifact of the underestimation of the band gap by the LDA, and in practice the system is likely to be insulating, it does preclude the calculation of piezoelectric constants in this case. However calculations for MnO in the wurtzite structure indicate a large piezoelectric response (around 30 % larger than that of ZnO) which augurs well for piezoelectricity in the mixed systems[35].

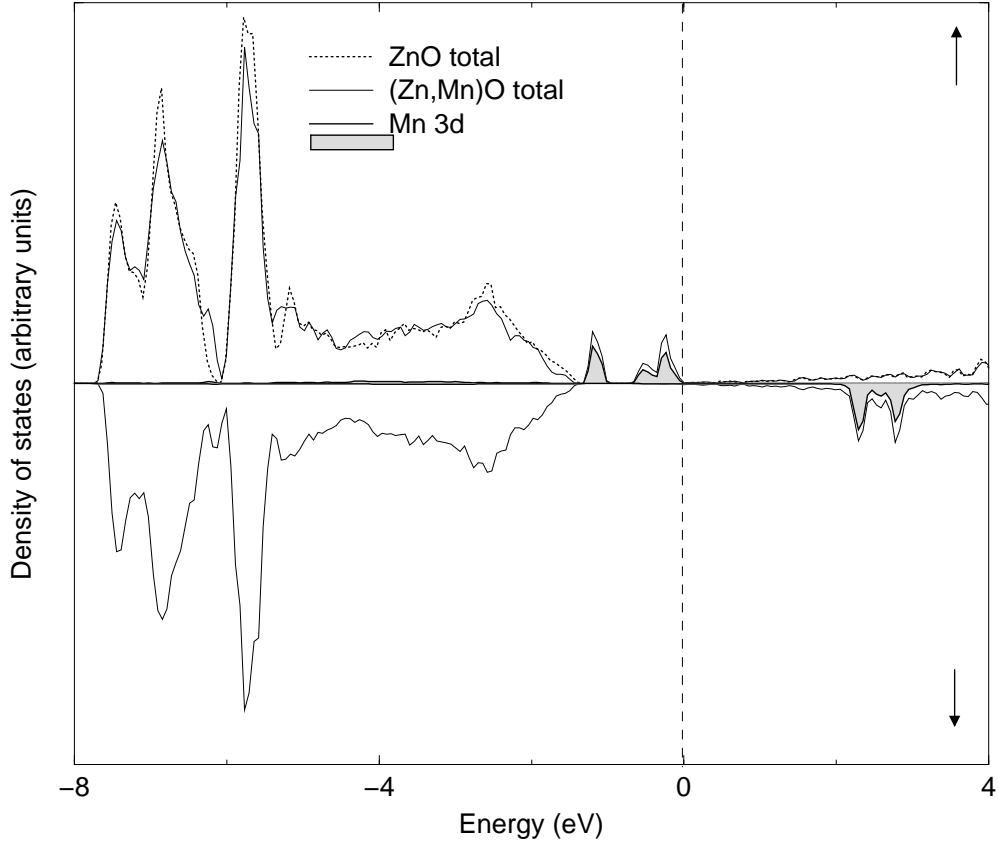


Figure 1: Calculated density of states in ferromagnetic (Zn,Mn)O with a manganese dopant concentration of 6.25 %. The solid line is the (Zn,Mn)O total density of states and the gray shading indicates the contribution from the Mn 3*d* orbitals. The positive *y* axis shows the majority (up) spin states and the negative *y* axis the minority (down) spin states. The ZnO total density of states is shown with a dashed line in the majority sector for comparison.

When two Mn atoms are included in a 32 atom unit cell (giving a 12.5 % doping concentration), a number of different magnetic and positional arrangements are possible. Here we adopt two different pairs of Mn positions; the ‘close’ configuration, in which the Mn ions in the same unit cell are separated by a single O ion, and the ‘separated’ configuration in which they are connected via -O-Zn-O- bonds. For both configurations we calculate the relative energies of the ferromagnetic and antiferromagnetic spin alignments. Note that our calculations show that the close configuration is more energetically favorable than the separated one by around 10 meV, suggesting that the Mn ions are likely to cluster together during growth, rather than distribute themselves evenly throughout the lattice.

In all cases the energy differences between ferro- and antiferromagnetic alignment are small (of the order of meV) with the antiferromagnetic state being more favorable for the separated configuration and the ferromagnetic being more favorable for the close configu-

ration. Note that these energy differences are so small that we believe that they are not significant within the uncertainties of the DFT calculation. We therefore predict that, in the absence of additional carriers or impurities, substitution of Zn by Mn ions in ZnO will produce paramagnetic behavior down to low temperature. This is in agreement with the earlier DFT calculations on this system[12, 13].

Next we simulate *n*-type doping by removing an oxygen atom to form an oxygen vacancy, as far as possible from the Mn ions. We find that this stabilizes the antiferromagnetic state for both close and separated configurations, but again by only one or two meV. In contrast, the incorporation of a Zn vacancy, representing *p*-type doping, stabilizes the ferromagnetic state of both configurations by significant amounts - the separated configuration by around 10 meV, and the close configuration by 60 meV - over the antiferromagnetic state. Notice that, in this case, there are free carriers in the system, and so the resulting metallicity will not allow piezoelectricity to occur. In the next subsection we analyze in detail why the introduction of *p*-type carriers stabilizes the ferromagnetic phase.

3.2 (Zn,Co)O

Next we repeat the calculations described in Section 3.1, but with Co instead of Mn as the magnetic dopant ion. Again we begin with a 32 atom unit cell containing a single Co atom, and consequently having ferromagnetic ordering. The density of states is shown in Figure 2 (a). The majority spin Co *d* states are lower in energy than their Mn counterparts and so are more strongly hybridized with the O 2*p* states at the top of the valence band. As in the case of Mn, the up-spin Co *d*-states are fully occupied. However, in contrast to the formally d^5 Mn^{2+} , in the case of formally d^7 Co^{2+} , the down-spin *d* states are also partially occupied, with the Fermi level lying in a gap between the crystal field split *e* and *t*₂ states. This arrangement occurs because the exchange splitting (between up-spin (↑) and down-spin (↓) states) is around 2 eV, while the crystal field splitting (between *e* and *t*₂ states) is much less than 1 eV. The d^7 configuration is therefore $e(\uparrow)^2, t_2(\uparrow)^3, e(\downarrow)^2, t_2(\downarrow)^0$, as sketched in Figure 3. (Note that in the Mn-doped compound, the crystal field splitting was even smaller (around 0.5 eV) and the exchange splitting larger (at around 2.5 eV)). The magnetic moment per unit cell is calculated to be 3.10 μ_B , close to the value of 3.0 μ_B predicted for purely ionic Co^{2+} .

When two Co atoms are included in a 32 atom unit cell (giving a 12.5% substituent concentration) we find that, for both close and separated configurations, the energies of the FM and AFM configurations are similar. This time, the FM is slightly lower (the energy of the separated FM configuration is 4 meV lower than that of the separated AFM separated configuration, and for the close configuration the FM is only 1 meV lower than the AFM). Again we believe that these small energy differences, which would anyway correspond to Curie temperatures of the order of around 10 to 40 K, are not significant within the uncer-

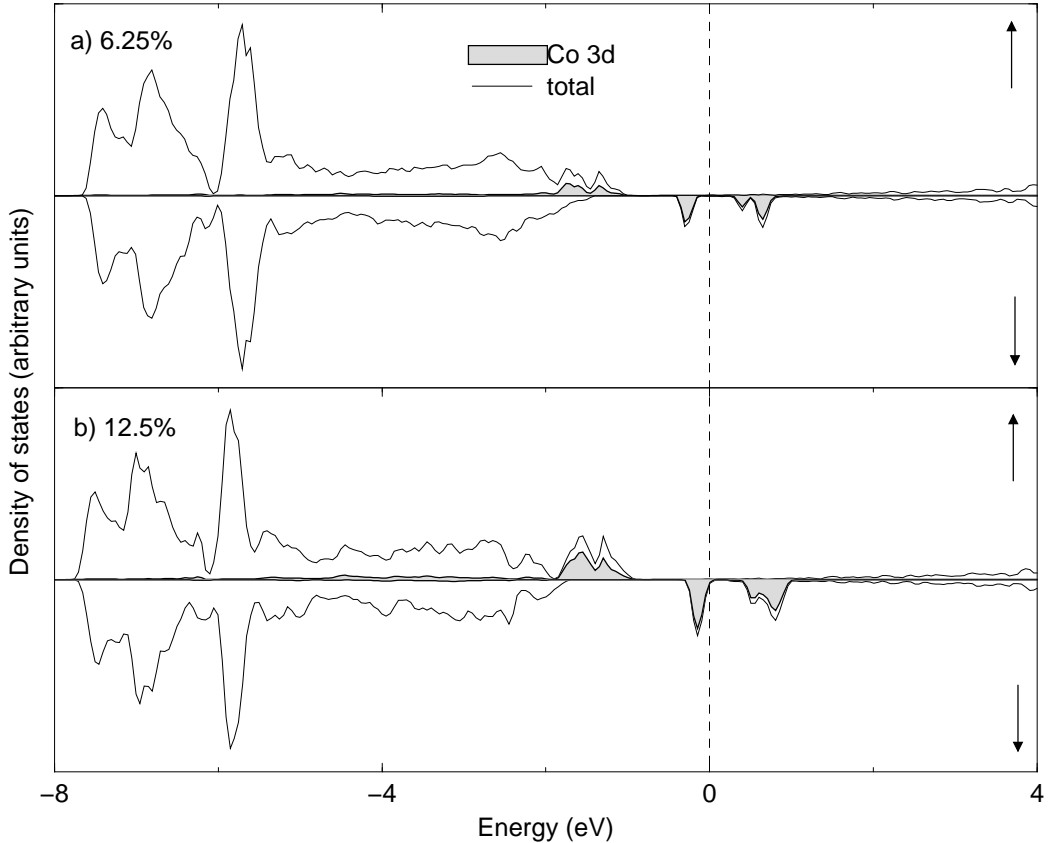


Figure 2: Calculated densities of states in ferromagnetic $(\text{Zn,Co})\text{O}$ with cobalt dopant concentrations of (a) 6.25 % and (b) 12.5 %. The thin solid lines show the $(\text{Zn,Co})\text{O}$ total densities of states and the thick solid lines with the gray shading indicate the contribution from the Co 3d orbitals. Majority spin states are plotted along the positive y axis, and minority spin along $-y$.

tainties of the DFT calculation. Our results are in sharp contrast to earlier calculations[12] which predicted the ferromagnetic state to be 200 meV lower than the antiferromagnetic in $(\text{Zn,Co})\text{O}$, corresponding to a ferromagnetic Curie temperature of around 2000 K.

The calculated density of states of the 12.5 % doped ferromagnetic system, with the Co atoms separated, is shown in Figure 2 (b). The structure is similar to that at 6.25 % doping except for a broadening of the Co bands as expected. The total magnetic moment per unit cell is $6.1 \mu_B$ for both close and separated configurations, again close to the ideal ionic value of $3.0 \mu_B$ per ion for high spin Co^{2+} .

Again we have modeled hole doping in our system by removing a Zn atom from the 32 atom unit cell of 12.5 % substituted $(\text{Zn,Co})\text{O}$. Such p -type doping strongly stabilizes the FM state. In both the separated and close configurations the FM state is now 60 meV lower in

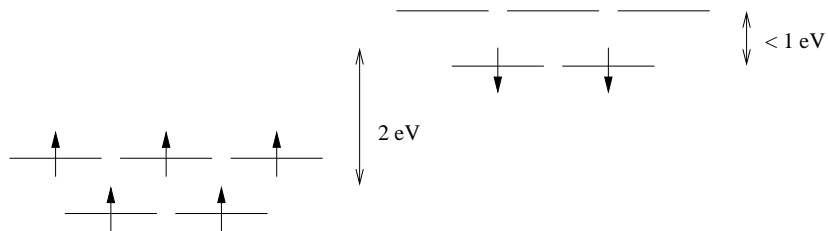


Figure 3: Schematic energy diagram for a Co^{2+} ion in a tetrahedral oxide ligand field. The exchange splitting of around 2 eV is considerably larger than the crystal field splitting (less than 1 eV).

energy than the AFM state. The magnetic moment increases to $8 \mu_B$ per unit cell ($4 \mu_B$ per Co), up from the value of $6.1 \mu_B$ for the un-doped case. This is consistent with the removal of two minority spin electrons from each supercell. Note however that Mulliken population analysis reveals that this additional magnetic moment in fact resides on the oxygen atoms rather than being localized on the Co ions. The occupation of the Co d states is 5 up-spin electrons and 2.4 down-spin electrons in both ferro- and antiferromagnetic cases. (Of course the AFM case has a complementary Co ion with 5 down-spin and 2.4 up-spin electrons.) It is also notable that the minority electrons are distributed approximately evenly between all five d orbitals. This indicates that the interaction with the hole states causes strong ligand field effects which overcome to some extent the crystal field splitting into occupied e and empty t_2 minority states.

The densities of states for both the ferro- and antiferromagnetic hole-doped systems are shown in Figure 4. Note that the y -axis has been expanded compared with those in the earlier figures, so that the Co states occupy most of the range. The two Co ions in each unit cell are plotted separately, one shown by a thick solid line and one by a thick dotted line. In both cases, as expected, the Fermi energy is shifted down relative to the broad oxygen $2p$ band compared with the undoped cases. (Since E_F is set to 0 eV, this is manifested by a shift up in energy of the bottom of the valence band). We see that the majority electrons on each Co ion hybridize very strongly with the oxygen p states, giving a broad band with a width comparable to that of the O p band. The increase in hybridization compared with the undoped case is notable. Also striking in comparison with the undoped case is the mixing of the minority spin electrons with the oxygen band. Although the differences between the FM and AFM electronic structures are indeed subtle, the FM arrangement seems to allow for stronger energy-lowering hybridization seen in the slightly broader bandwidth compared with the AFM case. Also the FM arrangement allows a gap opening at the Fermi energy which might contribute to its stabilization. Note however that the gap is vanishingly small, and so any piezoelectric response would be expected to be rather lossy.

In contrast, if the vacancy is created on the anion site (O atom replaced by a \square), the

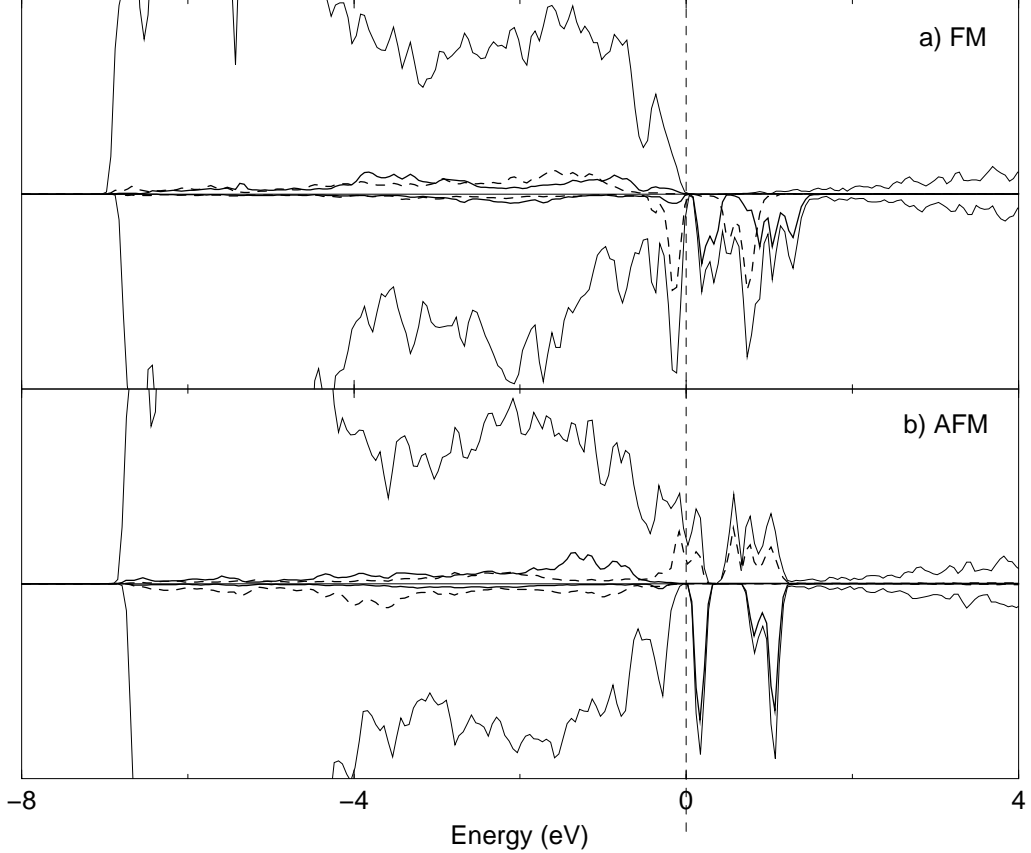


Figure 4: Calculated density of states in a) ferromagnetic and b) antiferromagnetic $(\text{Zn,Co})\text{O}$ with a cobalt dopant concentration of 12.5 % (Co ions in the separated configuration) and a single Zn vacancy. The thin solid line is the $(\text{Zn,Co})\text{O}$ total density of states and the thick black solid and dashed lines indicate the contributions from the $3d$ orbitals on each Co ion separately.

resulting n -doping stabilizes the AFM state. In the n -doped separated configuration, the AFM state is now 4 meV lower in energy than the FM, and for the close configuration the AFM state is 1 meV lower than the FM.

3.3 ZnO with vacancies

Finally for this section, we investigate the intriguing possibility that a ferromagnetic state could be obtained in a simple oxide solely from interactions between vacancies[36]. First we introduce a single Zn vacancy into our 32 atom unit cell, and initialize our calculation with the two oxygen atoms adjacent to the vacancy polarized either parallel or antiparallel to each other. The two starting conditions converge to different final solutions with magne-

tizations of $1.8 \mu_B$ and $0.4 \mu_B$ per supercell. A fully antiferromagnetic solution, with total magnetization of $0.0 \mu_B$, is not obtained. The energy of the more spin-polarized solution is lower than that of the less polarized by 100 meV. Next we repeat the calculation with *two* Zn vacancies. Again two spin-polarized solutions are obtained, one with a magnetization of $2.9 \mu_B$ per unit cell, and the other with $0.6 \mu_B$ per supercell, and again the more spin-polarized solution is lower in energy by 100 meV per supercell. Although we cannot guarantee the absence of other (possibly AFM) minima, our results do suggest that solutions with larger spin polarization have lower energy in such vacancy-doped systems. Note however that the vacancy concentrations in both cases studied here are much larger than realistic experimental values.

4 Summary and future work

Our results suggest that, in contrast to earlier predictions, robust ferromagnetism will only be obtained in transition metal doped ZnO if *p*-type carriers are also included. The method that we employed computationally, namely imposing a high concentration of Zn vacancies, is clearly unfeasible experimentally. In fact, *p*-type ZnO is notoriously difficult to realize, although there have been successes reported using co-doping techniques [37]. In this final section we propose that doping with Cu should be a feasible way of making ZnO *p*-type. A relativistic Cu pseudopotential, generated from a $4s^1 3d^{10}$ ground state with r_{cs} of 2.1 a.u. for each orbital and partial non-linear core corrections was used. A double zeta plus polarization basis for $4s$ and $4p$ orbitals, and triple zeta plus polarization for $3d$, with confinement radii of 7.0, 7.0 and 6.5 a.u., gave identical lattice constants, bulk modulus and band structure for bulk Cu to those of plane wave and ultra-soft pseudopotential calculations.

We performed a total energy calculation for a 32 atom unit cell in which one Zn atom was replaced by a Cu atom. Mulliken population analysis indicated a total valence charge on the Cu atom of 10.3, compared to the ideal values of 10 for Cu^+ or 9 for Cu^{2+} . This suggests that the Cu is adopting close to a +1 ionization state when it substitutes for a Zn^{2+} ion, indicative of *p*-type doping. Figure 5 shows the total density of states for the system, with the Cu $3d$ partial density of states highlighted. Note that the “acceptor” state above the Fermi energy is broader than that seen in a prototypical *p*-type semiconductor band structure because the dopant concentration considered here is much higher. It is clear that the up-spin Cu states are completely filled, as expected, with the down-spin states almost filled, giving a half-metallic band structure. As a result of the half-metallicity, the magnetic moment corresponds to an integer number of Bohr magnetons and is equal to $1 \mu_B$. About half of the moment is carried in the Cu $3d$ states (the Mulliken distribution of the Cu charge between its atomic orbitals is $3d_{\uparrow}^{5.0} 3d_{\downarrow}^{4.5} 4s_{\uparrow}^{0.177} 4s_{\downarrow}^{0.175}$), with the remainder delocalized across its oxygen nearest neighbors. Note that these results were obtained within the LSDA, and more detailed studies using beyond-LDA methods are ongoing.

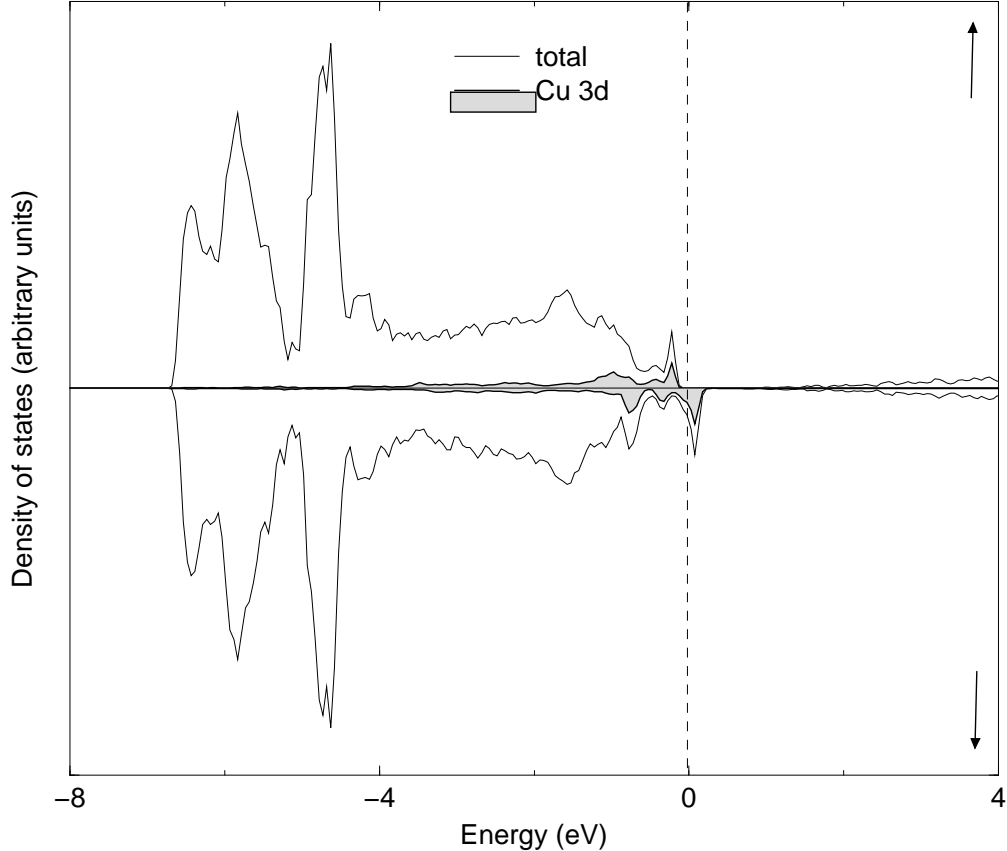


Figure 5: Calculated density of states in (Zn,Cu)O with a copper dopant concentration of 6.25 %. The solid line is the (Zn,Cu)O total density of states and the gray shading indicates the contribution from the Cu 3d orbitals. Majority spin states are plotted along the positive y axis, and minority states along negative y .

Finally, we calculate the effect of simultaneously doping with both Co and Cu, in the expectation that the p -type doping from the Cu will induce ferromagnetic interactions between the Co ions. We find this indeed to be the case. When two separated Co ions are included in a 32 atom unit cell with a single Cu ion (placed as far as possible from the Co ions) we obtain a ferromagnetic ground state which is over 80 meV lower in energy than the corresponding antiferromagnetic state. Note that there has been a recent experimental report of Cu-doping inducing ferromagnetism with a Curie temperature of 550K in otherwise paramagnetic Fe-doped ZnO[38]. The authors attribute the ferromagnetism to the presence of Cu^+ ions (observed by x-ray absorption spectroscopy), although in this case Hall effect measurements indicate that the sample is strongly n -type.

In conclusion, our density functional theory calculations indicate that ferromagnetism can indeed be obtained by substituting Zn in ZnO with either Co or Mn, but that it will only occur in the presence of simultaneous p -doping. We also propose a realistic scheme

- the incorporation of Cu^+ ions on the Zn sites - for achieving the p -doping. Although our results are encouraging for the production of ZnO-based ferromagnets, they do not augur well for straightforward production of a ZnO-based magnetic piezoelectric, since the additional carriers required to stabilize the ferromagnetic state will be detrimental to the piezoelectricity.

5 Acknowledgments

NAS thanks David Clarke and Ram Seshadri for discussions regarding suitable possible dopants for creating p -type ZnO. This work was supported by the Department of Energy, grant number DE-FG03-02ER45986, and made use of MRL central facilities, supported by the the National Science Foundation under the Award No. DMR00-80034. NAS thanks the Earth Sciences Department at Cambridge University for their hospitality during the sabbatical leave in which the calculations were performed.

References

- [1] H. Ohno, *Science* **281**, 951 (1998).
- [2] S.A. Wolf, D. D. Awschalom, R. A. Buhrman, J. M. Daughton, S. von Molnar, M. L. Roukes, A. Y. Chtchelkanova and D. M. Treger, *Science* **294**, 1488-1495 (2001).
- [3] V.E. Wood and A.E. Austin, in *Magnetolectric interaction phenomena in crystals*, eds. A.J. Freeman and H. Schmid, Gordon and Breach, 1975.
- [4] T. Dietl, H. Ohno, F. Matsukura, J. Cibèrt and D. Ferrand, *Science* **287**, 1019 (2000)
- [5] A. Risbud, N.A. Spaldin, Z.Q. Chen, S. Stemmer and R. Seshadri, submitted to *Phys. Rev. B*.
- [6] K. Ando, H. Saito, Z. Jin, T. Fukumura, M. Kawasaki, Y. Matsumoto and H. Koinuma, *J. Appl. Phys.* **89**, 7284 (2001).
- [7] K. Ando, H. Saito, Z. Jin, T. Fukumura, Y. Matsumoto, A. Ohtomo, M. Kawasaki and H. Koinuma, *Appl. Phys. Lett.* **78**, 2700, (2001).
- [8] K. Ueda, H. Tabata and T. Kawai, *Appl. Phys. Lett.* **79**, 988 (2001).
- [9] J. H. Kim, H. Kim, D. Kim, Y. E. Ihm and W. K. Choo, *Physica B* **327**, 304 (2003).

- [10] Z.-W. Jun, T. Fukumura, K. Hasegawa, Y.-Z. Yoo, K. Ando, T. Sekiguchi, P. Ahmet, T. Chikyow, T. Hasegawa, H. Koinuma and M. Kawasaki, *J. Crystal Growth* **237-239**, 548 (2002).
- [11] S.-W. Lim, D.-K. Hwang and J.-M. Myoung, *Solid State Commun.* **125**, 231 (2003).
- [12] K. Sato and H. Katayama-Yoshida, *Jap. J. Appl. Phys. II Lett.* **39**, **6B**, L555-L558 (2000).
- [13] K. Sato and H. Katayama-Yoshida, *Phys. Stat. Sol. B* **229**, 673 (2002)
- [14] P. Ordejón, D. Sánchez-Portal, E. Artacho and J.M. Soler, SIESTA, Spanish Initiative for Electronic Simulations with Thousands of Atoms
- [15] D. Sánchez-Portal, P. Ordejón, E. Artacho and J.M. Soler, *Internat. J. Quantum Chem.* **65**, 453-61 (1997) and references therein
- [16] P. Ordejón, *Phys. Stat. Sol. B* **217**, 335-56 (2000)
- [17] S. Sanvito, P. Ordejon and N.A. Hill, *Phys. Rev. B* **63**, 165206 (2001).
- [18] N. Troullier and J.L. Martins, *Phys. Rev. B* **43**, 1993 (1991)
- [19] S.G. Louie, S. Froyen and M.L. Cohen, *Phys. Rev. B* **26**, 1738 (1982)
- [20] L. Kleinman and D.M. Bylander, *Phys. Rev. Lett.* **48**, 1425 (1982)
- [21] D.M. Ceperley and B.J. Alder, *Phys. Rev. Lett.* **45**, 566 (1980).
- [22] A. dal Corso, M. Posternak, R. Resta and A. Baldereschi, *Phys. Rev. B* **50**, 10715 (1994).
- [23] *Semiconductors Physics of Group IV elements and III-V Compounds*, edited by K. H. Hellwege and O. Madelung, Landolt-Börnstein, New Series, Group III, Vol.17, Pt.a (Springer, Berlin 1982); *Intrinsic Properties of Group IV Elements and III-V, II-VI, and I-VII Compounds*, edited by K. H. Hellwege and O. Madelung, Landolt-Börnstein, New Series, Group III, Vol.22, Pt.a (Springer, Berlin 1987).
- [24] S. Sanvito and N.A. Hill, *Phys. Rev. B* **62**, 15553 (2000).
- [25] N. A. Hill and U. Waghmare, *Phys. Rev. B* **62**, 8802-8810 (2000).
- [26] N.A. Hill, *J. Phys. Chem. B.*, **104**, 6694-6709 (2000).
- [27] E. Artacho, D. Sanchez-Portal, P. Ordejón, A. García and J.M. Soler, *Phys. Stat. Sol.* **215**, 809 (1999)
- [28] K. Goto, N.A. Spaldin and S. Sanvito, in preparation

- [29] E.G. Moroni, G. Kresse, J. Hafner, Phys. Rev. B **56**, 15629 (1997).
- [30] J. Junquera and P. Ghosez, Nature **422**, 506 (2003).
- [31] J.P. Perdew and A. Zunger, Phys. Rev. B **23**, 5048-5079 (1981).
- [32] D. Vogel, P. Krüger and J. Pollman, Phys. Rev. B **52**, R14316-9 (1995).
- [33] A. Svane, W.M. Temmerman, Z. Szotek, J. Lagsgaard and H. Winter, Int. J. Quant. Chem. **77**, 799-813 (2000).
- [34] D. Vogel, P. Krüger and J. Pollman, Phys. Rev. B **52**, R14316-9 (1995).
- [35] P. Gopal and N.A. Spaldin, in preparation.
- [36] I. S. Elfimov, S. Yunoki, and G. A. Sawatzky Phys. Rev. Lett. **89**, 216403 (2002).
- [37] M. Joseph, H. Tabata and T. Kawai, Jpn. J. Appl. Phys. **38**, L1205 (1999).
- [38] S.-J. Han, J.W. Song, C.-H. Yang, S.H.Park, J.-H. Park, Y.H. Jeong and K.W. Rhie, Appl. Phy. Lett. **81**, 4212 (2002).